Reasoning about Fluid Motion I: Finding Structures

Kenneth Yip *
Department of Computer Science
Yale University
P.O. Box 208285, Yale Station
New Haven, CT 06520-8285.
(yip-ken@cs.yale.edu)

Abstract

With the increasing role of high performance computing in attacking complex physical problems, there is an urgent need for the development of advanced computational technology to provide scientists with high-level assistance in the analysis, interpretation, and modeling of a massive amount of quantitative data. A critical area where this need is quite evident is the problem of turbulence. The overall research goal is to develop a computational environment to help scientists efficiently make observations and conceptual models of turbulence data sets. This paper presents the progress of this project. My approach is based on two key ideas: (1) Local interactions and evolution of coherent objects like vortices enable high-level qualitative interpretation of turbulence data, and (2) Abstracting from the particular features of fluid dynamical reasoning, 1 propose five core operations - aggregation, classification, re-description, spatial inference, and configuration change - as part of a general theory of imagistic reasoning. A new vortex-finding algorithm is also presented.

"Feymann said ... when Einstein stopped creating it was because he stopped thinking in concrete physical images and became a manipulator of equations."

Genius, James Gleick, p244, 1992.

1 Introduction

It is commonly believed that there are two styles of scientific thinking: *analytical,* a logical chain of symbolic reasoning from premises to conclusions, and *visual,* the holding of imagistic, analogue representations of a problem in one's mind so that perceptual and symbolic operations can be brought to bear to make deductions. Neither style is to be preferred a priori over the other. However, for problems whose complexity precludes a direct analytical approach, a certain amount of qualitative and visual imagination is needed to provide the necessary "feel" or "understanding" of the physical phenomena. Once the picture is clear, the analytical mathematics can take over and lead more efficiently to logical conclusions.

This "feel and physical understanding" is rather informal, imprecise, and apparently unteachable, but necessary for scientists. My research goal is to formalize the visual style of thinking as computer programs, and to demonstrate the power of these programs by their ability to reason about the structure and motion of turbulent fluid flows.

The choice of fluid flows as a domain may seem arbitrary and turbulence may add unnecessary difficulty to the project. However I believe the subject matter is fascinating, ripe for attack, more constrained than a commonsense theory of liquids, and, most importantly, is worthwhile because new tools for advancing turbulence research can have enormous scientific values.

Turbulent flows have been studied for many decades. But only recently has the capacity to perform direct numerical simulation (DNS) of turbulent flows at moderate Reynolds numbers with enough accuracy been realized. [1] So for the first time detailed solution fields are available to scientists. Some of the important questions facing scientists are: How does one make observations from the data? How does one make theories based on new observations? How are data used to test theories?

Currently there is a large effort in Scientific Visualization whose goal is to develop computer graphics to facilitate the presentation of large datasets. However the process of discovering interesting structures in the datasets and extracting physics from them is up to the human experts. Even with the help of modern visualization software (such as AVS and Explorer), most human

* The research was funded in part by NSF NYI Award ECS-9357773.

'The terminology is explained in sections 2 and 3.

experts find the task time-consuming and prone to human visualization error. [2]

In collaboration with experts in fluid dynamics from Yale and MIT, I am building computer tools that can reduce the post-processing time of CFD data by orders of magnitude. My approach is based on the following key idea: Active Visualization and Abstraction (AVA). [3] By "active" I mean the reasoning process has three properties:

- *Autonomous* - the computer holds pictures in its mind so that perceptual operations can be used to make inferences which are otherwise too difficult to make by analytical methods alone.
- *Purposeful* - the visualization is done in the context of making observations and testing theories.
- *Generative* - the results of visualization guide the computer to make further observations.

By abstraction, I mean the process of reducing the encoding length of the datasets. A moderate-sized instantaneous flow field might consist of $O(10^7)$ grid points each with a 4-vector (three components for velocity and one for pressure) associated with it. It is hard to imagine four numbers or even one at each point of space. Could we re-represent the flow field by semi-persistent objects that are much more compact and easy to visualize? That the physical picture of moving and deforming objects, called vortices, is a useful level of abstraction for reasoning about fluids is an important claim of AVA.

What does AVA consist of? I conjecture that AVA consists of five core operations: [4]

1. Aggregation
2. Classification
3. Re-description
4. Spatial inference
5. Configuration change

Aggregation is the grouping of primitive objects according to some measure of similarity (e.g., closeness, continuity, symmetry). For a familiar example, consider a vector field. Points in the vector field can be grouped into integral curves or orbits. Classification is the assignment of labels to the aggregate objects. Each label denotes a bundle of characteristic properties. Re-description gives a more concise representation of the aggregate. These aggregates might possess character-

further discussion of this issue and current approaches in the visualization literature can be found in [Samtaney *et al,* 1994].

[3]The concept is similar in spirit to the idea of "active vision" in the vision literature, which means the active control of camera movements and focus of attention to improve the robustness and stability of vision. I apply the concept to a higher-level cognitive process.

[4]These core operations are distilled from a rethinking of how phase space analysis programs - like KAM [Yip, 199l] or MAPS [Zhao, 1994] - work. I suspect much of the work in mechanism analysis using configuration space (e.g. [Joskowicz and Sacks, 1991]) can be cast in the same framework.

istic shape and might touch or overlap. Deduction of these geometric relations is the province of spatial inference. The characteristic properties of an object might constrain what other objects can exist or change or deform in its neighborhood. Finally, the whole cycle of core operations can be reapplied at a more abstract level.

A word about related works. Commonsense reasoning about fluids is a central problem in naive physics [Hayes, 1985b; 1985a]. The problem is hard because fluids do not conveniently divide into discrete pieces that can be easily combined. Ken Forbus and his group have done important work in extending and partially implementing Pat Hayes' ideas for representing fluids using both the contained-liquid and piece-of-stuff ontologies [Forbus, 1984; Collins and Forbus, 1987]. The work described here is closer to the scientific end of the formalization spectrum. As a consequence the theory is less general than Hayes' theory, but more relevant to the research in the turbulence community. I expect the two lines of research to have fruitful interactions.

2 Properties of fluid motion

A fluid is either a gas or a liquid; it is not a solid. The behavior of fluid is interesting and often surprising. One can get a good understanding of fluids by thinking about the properties of water. Solids resist deformation; fluids yield to any shear stress. Solids care how far they deform; fluids how fast they deform. The measure of the ease of deformation is *viscosity.* A more viscous fluid like honey deforms more slowly than a less viscous one like water. If the fluid is not moving, the only force it exerts is pressure, which always acts in the direction normal to any surface in the fluid. If the fluid is moving, a number of new forces come into play. Viscosity, an internal friction so to speak, causes a shear stress to develop between layers of fluid moving in different velocity. A fluid moving across a solid surface tends to *drag* the surface with it. This property is known as the no-slip condition, i.e., the velocity of the fluid is exactly zero at the solid surface. The frictional forces always act in the opposite direction of motion. A fluid moving over an asymmetrical solid surface can create *lift,* a force perpendicular to the direction of motion.

Real fluids are quite complicated, so I will make some assumptions about the properties of the flow to simplify the discussion. The assumptions are convenient fictions, but in many interesting cases they are rather good approximations:

1. Fluids are incompressible. This is really the conservation of mass. The volumetric flow rate is the same at every point in the fluid; no fluid can accumulate anywhere.

2. Fluids are Newtonian. This gives a particularly simple linear relationship between the applied shear stress and the rate of deformation.

3. No temperature variation, Coriolis forces, nor electromagnetic forces exist that might affect the fluid. The Newtonian, incompressible fluid is already complicated enough.

The payoff of these assumptions is large. The only relevant forces on the fluid, besides pressure, are inertial and viscous. The inertial forces keep the fluid going; the viscous try to stop it. The ratio between the two forces, a dimensionless number, is called the *Reynolds number,* denoted by the symbol Re.

One reason why the Reynolds number is an important parameter is that the character of fluid motion is strongly dependent on it. A very high Reynolds number flow (Re >► 1000) is dominated by inertial forces and tends to favor *turbulence* in which individual "fluid particles" move in a random unpredictable fashion even when the fluid as a whole is moving in a definite direction. Large viscous forces such as those in a flow with very low Reynolds number should damp turbulence and maintain a *laminar flow* in which fluid particles move more or less parallel to each other. In between the very high and very low Reynolds number flows are the transition flows whose character depends on the circumstances.

To get an idea of the different regimes of a real fluid flow, consider a steady incompressible flow past a symmetric "bluff body" (a non-streamlined body such as a circular cylinder or a sphere). See Fig. 1. At very low Reynolds number, when the flow is slow, the flow pattern consists of smooth symmetrical *streamlines,* the trajectories of the fluid particles. As the Reynolds number is increased, a pair of symmetrical eddies or vortices appears in the rear of the cylinder where fluid particles curl around. If the flow speed continues to increase, the vortices become elongated and at some point break off, traveling downstream with the fluid. The phenomenon is known as *flow separation.* New vortices begin to form near the behind of the cylinder and shed alternatively into the cylinder wake. At sufficiently high Reynolds number, turbulence sets in and the wake begins to oscillate; the flow is unsteady and highly irregular. Vortices of many different length scales are also visible.

What really happens inside a turbulent flow? Is the motion of fluid particles purely random? Or is there organized motion within a background of smaller scale random fluctuation? Experimental evidence seems to favor the latter alternative. Nobody really knows for sure. But why do we care anyway? The reason is that although we do not understand turbulence, its effects are highly significant. Turbulence increases drag, mixing of materials, and transport of heat. In designing an air transport, we might want to suppress turbulence in order to reduce drag; in a combustion engine on the other hand we might want to enhance turbulence to increase mixing rate. If large-scale structures do exist inside a turbulent flow *and* are found to be responsible for the enhanced mixing and transport properties, then it might be possible to control

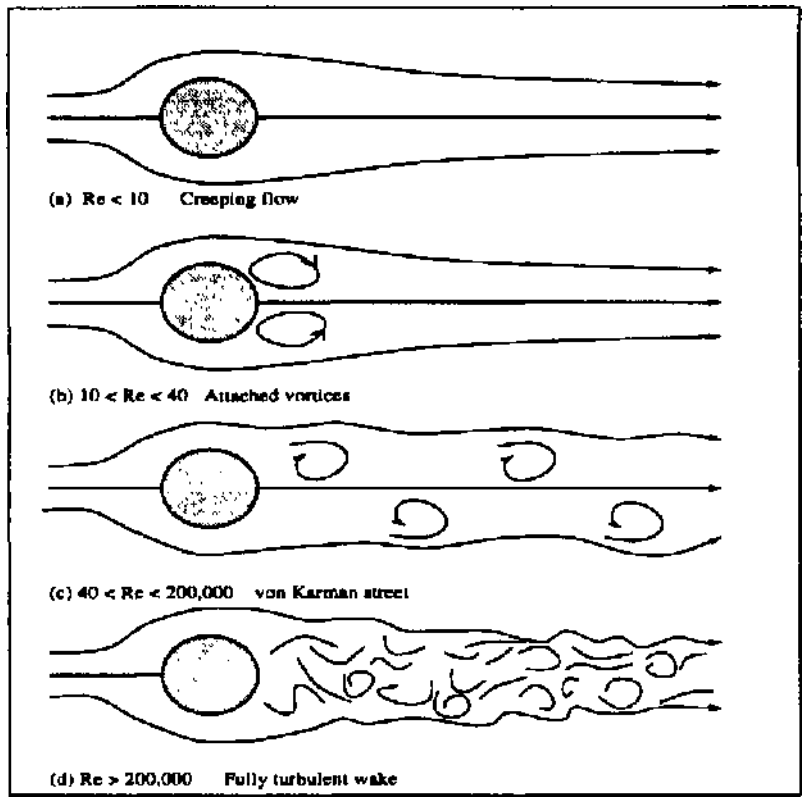

Figure 1: Schematic flow patterns around a circular cylinder, (a) Symmetrical streamlines and absence of vortices, (b) A pair of vortices in the rear of cylinder, (c) Alternating vortices shed downstream, (d) A turbulent wake with vortices of many length scales.

turbulence by direct interference with these structures.

3 Reasoning tasks

Given a numerical solution field of a turbulent flow, a spectrum of reasoning tasks can be defined. The following list is roughly in the order of increasing complexity:

1. Making observations. Find out structures, if any, that exist in the solution field. Are there vortices? What are their shapes and sizes? How are they distributed? How are they created? How do they evolve and interact?

2. Making correlations. Determine how the shape and distribution of structures correlate with fluid velocities, pressure, dissipation, and other statistical properties of the flow.

3. Incremental analysis. Given an instantaneous configuration of structures, predict the possible short-time behaviors.

4. Causal analysis. Explain and summarize the evolution of structures by a set of elementary interaction rules.

5. Testing theories. Given a hypothesis about structure formation or interaction, gather evidence to support or disprove the hypothesis.

4 Domain Theory

The entire theory of incompressible flow is contained in the *Navier-Stokes equations:*

$$\nabla \cdot \mathbf{u} = 0$$
$$\frac{\partial \mathbf{u}}{\partial t} + (\mathbf{u} \cdot \nabla)\mathbf{u} = -\nabla p + \nu \nabla^2 \mathbf{u}$$

The first equation expresses the conservation of mass; it is the incompressibility assumption. It says the velocity u, which has three components, has zero divergence. The name divergence is well-chosen for ▼-u is a measure of how much u spreads out (diverges). If it is positive (negative) at a point P, then P is a source (sink). Zero divergence means no source or sink inside the flow.

The second equation comes from Newton's second law of motion; it equates fluid acceleration with applied forces. The acceleration terms, the left hand side of the second equation, represent the change of velocity in time and space. On the right hand side, the first term —▼p is the pressure gradient. The second term, *u* is the *kinematic viscosity* which is the ratio of the viscosity and density of the fluid; the product of *v* and the second spatial derivatives of the velocity V^2u is the force due to viscosity.

Since we can associate with every point (x, y, *z)* in space and instance *t* with a velocity u, we call u(ar, y, z, *t)* a *velocity field.* A field is any physical quantity that takes on different values at different positions and time. *u(x,y, z,t),* like a magnetic field, is a vector field because at each space-time point, we associate a vector with three components. The pressure field *p(x,y, z,t)* like temperature is a scalar field - one number for each point.

While useful for some specialized flows, the velocity field and its topology are not a particularly good representation of turbulent flows. The velocity field not only is *not* Galilean invariant (what an observer sees depends on how fast she is moving), but also can change quite unpredictably from one instance to another. As a consequence, we cannot visualize what is happening - not easily. Just as some scientists prefer to think in terms of interaction of charges and magnets rather than the resulting magnetic field, many fluid dynamicists prefer to think in terms of a vector quantity called *vorticity,* denoted by the symbol w, which is the curl of the velocity, w= ▼x u. The curl of u at a point P measures how much the vector field u curls around P.

Suppose you float a paddlewheel on a bathtub. If it starts to turn, then the point it is placed has a non-zero curl. A region with a large curl is an eddy, a whirlpool. The curl of u is a vector; its direction is assigned by the right hand rule: if the water surface is the xy-plane and the paddlewheel turns counterclockwise, the curl points to the upward z-direction.

The reason we introduce the vorticity field w(x, *y, z, t)* is that it simplifies the description of fluid motion and gives ontological primitives which are easier to reason with. A vortex line is an integral curve of the vorticity field. The set of vortex lines passing through a simple closed curve in space is said to form the boundary of a *vortex tube.* Vortex lines and vortex tubes have nice invariant properties. In particular, they can be treated as material objects. The truth of this last statement follows from the so-called *Helmholtz laws of vortex motion.* For incompressible, *inviscid* (i.e., *v* = 0) flow, Helmholtz proved the following theorems [Batchelor, 1967]:

1. The vorticity field has zero divergence (because the divergence of a curl is always zero).

2. Vortex lines move with the fluid, i.e., fluid particles that at any time lie on a vortex line continue to lie on it.

3. The strength T of a vortex tube, defined as circulation $\Gamma = \int_S \omega \cdot ndS$ is the same for all cross-sections 5 of the vortex tube and is constant in time.

The first and second theorems explain why vortex lines or tubes can be treated as material bodies. The third theorem is just an expression of the conservation of angular momentum. The skater's spin is a nice illustration of the third theorem at work. By bringing in her arms and thereby shrinking the cross-section, the skater spins faster because the total angular momentum is conserved.

Turbulent flows are not inviscid, but at very high Reynolds number the viscous effect is very small except in a thin region close to the solid boundaries. So it is reasonable to expect the Helmholtz laws to be approximately correct.

Although the exact analysis of the motion of a configuration of vortex lines and vortex tubes can be very complicated, the simplest situations can be understood by a few qualitative principles:

Qualitative Rules of Vortex Motion

1. A vortex line accelerates velocity on one side and slows down on another. A lift force perpendicular to the vortex line is generated due to the Bernoulli effect.

2. A vortex line is convected by the fluid which exerts a drag force to push the vortex line in the direction of fluid motion.

3. A vortex tube stretched (compressed) in one direction increases (decreases) the velocity components in the other two directions.

4. A bent vortex line, conceptualized as a space curve, exerts a self-induced motion along its binormal and the effect is largest at points of maximum curvature [Arms and Hama, 1965].

5. Vorticity can only be created at velocity discontinuities and solid boundaries.

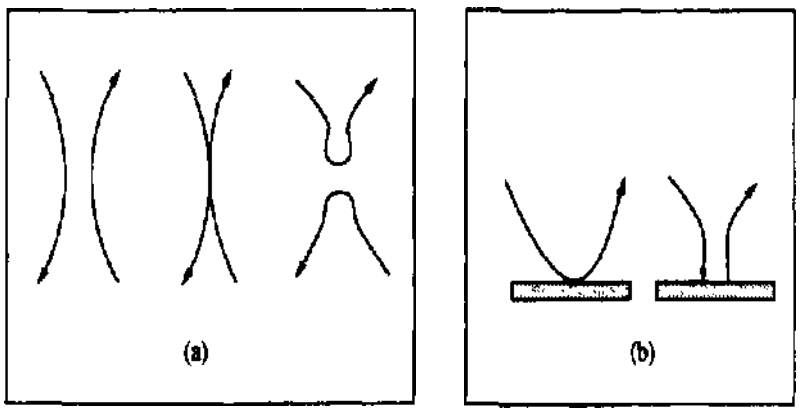

Figure 2: Motion of vortex lines can be understood by a few qualitative principles: Schematic pictures for two types of vortex line reconnection. (a) Two antiparallei vortex lines come together and reconnect to get rid of the region of opposing vorticity. (b) A similar reconnection occurs when a vortex line touches a free-slip boundary.

6. When two antiparallei vortex lines are brought close together, they can break apart and reconnect. (See Fig. 2)

7. When a vortex line meets a free-slip boundary, it can reconnect.

The first four rules are consequences of Helmholtz laws; they are good approximations even when applied to vortex tubes with finite core size as long as the core is relatively thin. The fifth is a kinematic consequence of the no-slip condition and the conservation of vorticity. The last two rules describe how the topology of vortex lines can change. The detail of the reconnection mechanism is still an open issue, but reconnection appears to happen experimentally.

The significance of these qualitative rules is that they allow the *synthesis* of the velocity field - at least the rotational component of the velocity. Main qualitative features of the flow field can often be deduced without complicated numerics. The use of these rules in incremental motion analysis will be the subject of a sequel paper.

5 Automatic Extraction of Vortex Structures

5.1 Aggregating vortex lines

A vortex line is the basic building block of a vortex structure. Because of the divergence-free property, a vortex line, like a magnetic field line, does not start or stop in the interior of the fluid; it tends to run in a closed loop. However, a real turbulent flow always has a background of randomly fluctuating vorticity. So it is reasonable to assume that only the relatively high-intensity vortex structures remain coherent from one time instance to another. To distinguish a "coherent" vortex from a mathematical vortex, I propose the following definition for aggregation:

Definition A *coherent vortex* is a compact bundle of adjacent, high-intensity vortex lines that are geometrically similar.

There is some degree of arbitrariness in any definition of coherent structure because the notion of coherence is informal. I believe the definition here is more faithful to the mathematical definition of a vortex tube. A coherent vortex can be tube-like or sheet-like depending on the shape of its cross-section. Unlike a mathematical vortex, a coherent vortex can start or end in the interior of the fluid.

Aggregating vortex lines to form coherent structures is not straightforward. Previous researchers [Moin and Kim, 1985; Robinson, 1991] have found that vortex lines are sensitive to initial conditions. Nearby vortex lines can diverge rapidly. If the initial conditions are not chosen carefully, the resulting vortex lines are likely to resemble badly tangled spaghetti wandering over the whole flow field, making the identification of organized structure extremely difficult. This might explain why vortex lines have not been widely used for structure identification. I believe the search algorithm below is the first successful structure identification based on vortex lines.

Given a numerical vorticity field, the search algorithm finds all coherent vortices. The key idea in the algorithm is the adaptive control of the cross-section of the vortex tube: the cross-section is shrunk (expanded) when the vortex lines on the boundary of the cross-section are converging (diverging). The algorithm has the following steps:

1. Find all grid points that are local extrema of vorticity magnitude and greater than a threshold. These are the seed points.

2. On the plane normal to the largest vorticity vector component at the seed point, find an isocontour centered at the point. The contour, discretized into points, represents the initial cross section of the surface.

3. Use the advancing front method (explained later) to interleave the advancement of the cross section by integration and the tiling of the surface.

4. Use the geometry of the tiles to decide shrinking or expanding the cross section locally.

5. The wavefront is periodically adjusted globally by computing its convex hull, and the diameter and width of the hull.

6. The forward integration terminates when the circulation on the cross section falls below certain threshold.

7. Reconstruct the surface by integrating the last cross section *backwards* until it reaches the initial cross

section. No wavefront adjustment is needed in this step.

8. Remove the weak vortex lines.

The advancing front method is implemented as follows. (See [Hultquist, 1992] for details.) The vortex surface consists of a list of ribbons. Each ribbon has two tracers: a left and a right. As its tracers are advanced, the ribbon is tiled by triangular meshes in such a way to keep wavefront nearly perpendicular to the integration direction. The aspect ratio of the quadrilateral formed by the last pair of alternating left and right triangles in each ribbon is used to control the local adjustment of the wavefront.

Vortex lines can twist and turn, so the cross sections can get distorted quite a bit as the surface is developed. The vortex-finding algorithm keeps track of the number of tracers. If the number exceeds a threshold, which is indicative of many highly distorted quadrilaterals, the entire cross section is replaced by the convex hull of the projected wavefront on a plane normal to the vorticity vector at the centroid of the cross section. The convex hull is useful for three purposes: (1) it reduces the number of tracers, (2) it re-orders the tracers into adjacent positions along the vertices of an oriented polygon, and (3) important shape information of the cross section such as its diameter and width can be computed in linear time from its convex hull [O'Rouke, 1994].

5.2 Aggregation results

As the test case, I use the DNS results of a free surface turbulence provided by Professor Dick Yue in the Ocean Engineering Department of MIT. The turbulence is generated by a shear flow in a 128^3 rectangular box with periodic boundary conditions in the x and y direction. A 4th order polynomial interpolation is used to compute the interpolated vorticity vector from the grid values, and an adaptive 4th order Runge-Kutta integrator to integrate vortex lines. Hundreds of structures have been constructed by the algorithm. A typical result is shown in Fig. 3a. The vortex is reconstructed from 10 vortex lines. The computation including rendering (done by AVS 5) takes about 90 seconds real time on a Sparc 10/51.

The algorithm is not sensitive to the initial choice of isocontour value: it is self-adjusting. Contrast this with an ordinary integrator. The vorticity lines obtained diverge and are tangled (Fig. 3b). Moreover, small changes in the initial isocontour can result in drastically different vortex line patterns.

5.3 Classification and Re-description

The reconstructed vortex must be interpreted in order to perform spatial inferences and incremental motion analysis. Classification is the assignment of labels to vortices. The assignment is determined by the shape of the vortex. A vortex can be tube-like or sheet-like. Tube-like

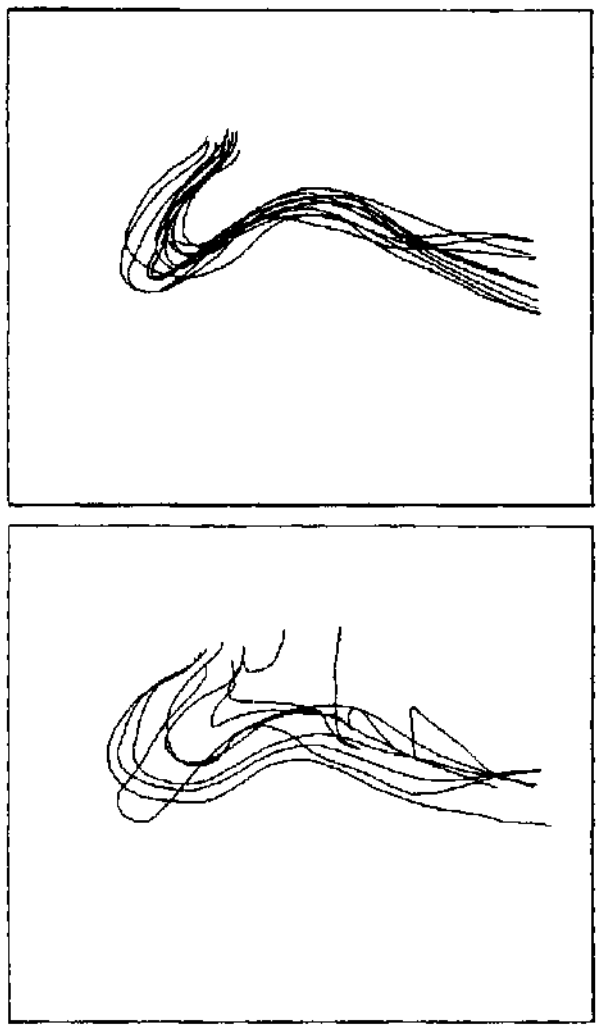

Figure 3: (a) Upper: A vortex structure reconstructed by the advancing wavefront method with backward integration. Each line is obtained by approximately 100 integration steps, (b) Lower: The vortex lines obtained by integration with no adaptive control of cross sections.

Figure 4: A generalized cylinder representation of the reconstructed vortex shown in Fig. 3a. The tiling is chosen to minimize twist between adjacent cross-sections.

vortices are further differentiated by the curvature function along their axes. It is important to identify the local curvature extrema because these extrema cause a self-induced motion (section 4).

To obtain a concise representation of a bundle of vortex lines, a vortex is re-described as a generalized cylinder (GC). A GC consists of a spline, a cross-section, and a sweeping rule [Binford, 1990]. The GC representation of a vortex is computed by the following steps:

1. Pick the vortex line with the highest integrated vorticity as the candidate spline.
2. Compute a scale-space representation of the curvature of the candidate spline [Witkin, 1983].
3. The stable local extrema are chosen as knot points.
4. At each knot point P, compute where the vortex lines intersect the plane at P with the plane normal equal to the vorticity vector at P.
5. Fit an ellipse to the intersection points to obtain a cross-section of the vortex.
6. The spline of the GC is obtained by spline-fitting the centers of the elliptical cross-sections.
7. Compute the intrinsic shape descriptions of the spline, i.e., its curvature and torsion.

By varying the criteria for stable curvature extrema, one can obtain generalized cylinders of different resolutions. Fig. 4 shows a rather fine generalized cylinder representation of the reconstructed vortex first shown in Fig. 3a.

6 Conclusion

This paper presents three novel ideas:

1. A zeroth-order formalization of the visual style of thinking as a cycle of five core operations: aggregation, classification, re-description, spatial inference, and configuration change.

2. A formalization of a theory of fluid flow based on new ontological primitives: vortex line, vortex tube, and coherent vortex, and a list of qualitative interaction rules.

3. A new vortex-finding algorithm based on vortex lines.

The implementation of spatial inference (such as determining spatial relations among vortices) and configuration change (such as incremental analysis of vortex motion) will be the subject of a sequel paper.

References

[Arms and Hama, 1965] R Arms and F.R. Hama. Localized-induction concept on a curved vortex and motion of an elliptic vortex ring. *Physics of Fluids,* 8, 1965.

[Batchelor, 1967] G.K. Batchelor. *An Introduction to Fluid Dynamics.* Cambridge University Press, 1967.

[Binford, 1990] T.O. Binford. Generalized cylinder representation. In *Encyclopedia of Artificial Intelligence.* Wiley, 1990.

[Collins and Forbus, 1987] John Collins and Kenneth Forbus. Reasoning about fluids via moecular collections. In *Proceedings AAAI-87,* 1987.

[Forbus, 1984] Kenneth D Forbus. Qualitative process theory. *Artificial Intelligence,* 24, 1984.

[Hayes, 1985a] Patrick Hayes. Naive physics 1: Ontology for liquids. In J.R. Hobbs and R.C. Moore, editors, *Formal Theories of the Commonsense World.* Ablex Publishing Corp., 1985.

[Hayes, 1985b] Patrick Hayes. The second naive physics manifesto. In J.R. Hobbs and R.C. Moore, editors, *Formal Theories of the Commonsense World.* Ablex Publishing Corp., 1985.

[Hultquist, 1992] J.P.M. Hultquist. Constructing stream surfaces in steady 3d vector fields. In *Proc. IEEE Visualization 92,* 1992.

[Joskowicz and Sacks, 1991] L Joskowicz and E.P. Sacks. Computational kinematics. *Artificial Intelligence,* 51,1991.

[Moin and Kim, 1985] P. Moin and J. Kim. The structure of the vorticity field in turbulent channel flow. *Journal of Fluid Mechanics,* 155, 1985.

[O'Rouke, 1994] Joseph O'Rouke. *Computational Geometry in C.* Cambridge University Press., 1994.

[Robinson, 1991] S.K. Robinson. The kinematics of turbulent boundary layer structure. Tech. Mem. 103859, NASA, 1991.

[Samtaney *et al.,* 1994]
R Samtaney, D Silver, N Zabusky, and J Cao. Visualizing features and tracking their evolution. *IEEE Computer,* July 1994.

[Witkin, 1983] Andrew Witkin. Scale-space filtering. In *Proceedings IJCAI-83.* International Joint Conference on Artificial Intelligence, 1983.

[Yip, 1991] Kenneth Yip. Understanding complex dynamics by visual and symbolic reasoning. *Artificial Intelligence,* 51, 1991. Special Volume on Qualitative Reasoning About Physical Systems II.

[Zhao, 1994] Feng Zhao. Extracting and representing qualitative behvaiors of complex systems in phase space. *Artificial Intelligence,* 69, 1994.

History-based Interpretation < f Finite Element Simulations of Seismic \ 5 Fields

Ulrich Junker
Institut Francois du Petrole

ILOG*
2, av. Gallieni, BP 85
94253 Gentilly Cedex
France
junker@ilog.fr

Bertrand Braunschweig
Institut Francais du Petrole
1 ct 4, av. de Bois-Preau, BP 311
92506 Rueil-Malmaison
France
Bertrand.Braunschweig@ifp.fr

Abstract

Dynamic objects such as liquids, waves, and flames can easily change their position, shape, and number. Snapshot images produced by finite element simulators show these changes, hut lack an explicit representation of the objects and their causes. For the example of seismic waves, we develop a method for interpreting snapshots which is based on Hayes[7] concept of a history.

1 Introduction

Most work on qualitative reasoning about physical systems is devoted to *technical systems* consisting of a fixed set of components that interact via given connections. Examples given in [Weld and de Kleer, 1990] are electronic circuits, water tanks, and gear systems. In contrast to this, we will consider *natural systems* where objects are *dynamic in position, direction, shape, and number.* The FROB system [Forbus, 1984] simulates springing balls changing their positions and directions, but keeping their shapes. Furthermore, we don't obtain new balls. Flowing liquids [Hayes, 1985a] are different: They easily divide, merge, and change their shapes. In order to capture those interactions between liquids, Hayes developed the concept of a history, i.e. a coherent piece of space-time. Histories provide an adequate means to describe the behaviour of *dynamic objects* such as flames, waves, clusters, clouds, which can all be deformed, divided and merged.

In this paper, we will consider a concrete task requiring history-based reasoning about physical phenomena. We consider the propagation of seismic shock waves in the underground [Lavergne, 1986]. Seismic waves are used by geophysicists to explore the structure of the underground. They are usually launched by an initial vibration on the surface. The resulting spheric shock wave is then propagating downwards as shown in the first snapshot of figure 1. When it hits an interface between two geological layers this causes a reflected and a transmitted wave. The reflected wave returns to the surface and leaves an observable front in the seismograms measured by the geophysicists.

In order to interpret seismograms, the geophysicists incrementally construct a model of the underground based on hypotheses of the histories of the returning waves. Above, we considered a wave that was reflected by the first interface. Further interfaces lead to further direct reflections. Additionally, a seismogram can show multiply reflected fronts, diffractions which are obtained due to corners and many other disturbing fronts. Geophysicists pick out direct reflections using some heuristic approach and use them to construct a model of the underground (based on numerical optimization procedures or further ad-hoc rules).

Newer work on numerical simulators based on finite elements allows a very precise simulation of the wave propagation in complex models of the underground. The snapshot sequence in figure 1 has been produced by such a simulator [Anne and Brae, 1994]. The simulations enable a verification of the geological model. Divergences between observed and simulated seismograms might help to correct the model. To detect them, we have to compare fronts having the same history (e.g. two direct reflections; two diffractions etc.). Unfortunately, numerical simulators based on finite elements do not keep track of the history of waves. They produce a series of images showing the waves, but they lack a representation of the wave objects, their causes, and their histories. When examining a front of a seismogram, we want to know the obstacles and the types of phenomena that produced it.

In this paper, we show how to *interpret* the images produced by the numerical simulator and how to establish a causal relation between seismic events, waves, and obstacles in the underground. Our goal is *to detect Hayes-like histories of waves in snapshot images.* Although the paper is restricted to 2D-models of the underground, its concepts can be generalized to the 3D-case.

The paper is divided into two main sections. Section 2 presents the representation of fields (sec. 2.1), as well as the vocabulary for describing wave histories (sec. 2.2). The interpretation is done in several steps developed in section 3. We first decompose the underground into layers and interfaces (sec. 3.1). Then we show how to detect

*This paper is based on work performed during the post-doctoral stay of the first author at the Institut Frangais du Petrole.

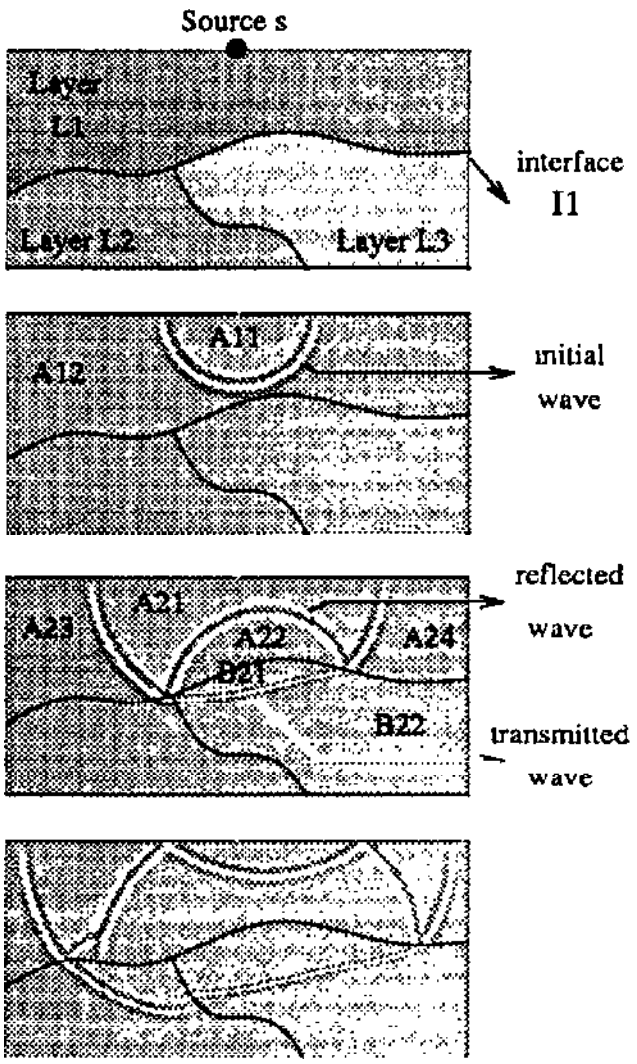

Figure 1: Snapshots of seismic waves.

wave fronts in a single snapshot (sec. 3.2). Tracking a front from one snapshot to the other is considered in section 3.3. In section 3.4, we discuss how to detect new objects and their causes.

2 Multiple representations

2.1 Fields

In order to describe complex phenomena (e.g. liquids, waves, flames etc.), physicists use parameter fields. A *field* is the distribution of a physical parameter in the given space. For shock waves, we consider a velocity field, giving the velocity of a wave at a certain point, and the field of the amplitudes of the waves (i.e. the snapshots in figure 1.). A *physical law* captures a relationship between parameter fields, which is valid at each point. In general, such a law is a differential equation (e.g. the wave equation). Its solution describes the temporal development of a field. Some of the fields such as the velocity field are static (stationary), whereas the amplitude field is changing in time (non-stationary). We restrict our discussion to a single static and a single dynamic field.

A well-suited technique for simulating changes of complex and arbitrary fields is the *funite element method.* A numerical simulator based on this technique is supplied

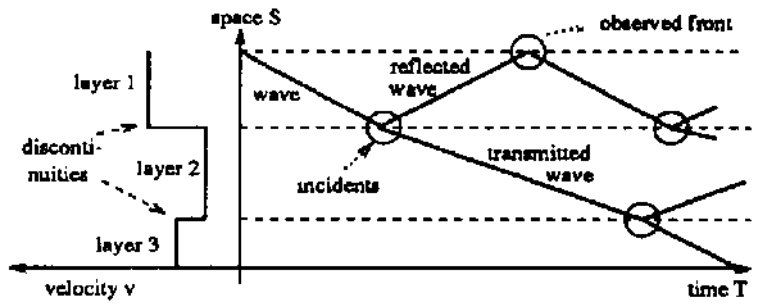

Figure 2: Dividing seismic histories into waves and incidents

with the initial parameter fields and then produces a series of snapshots showing the fields at selected instances of time. The finite element method can handle complex shapes because it uses a kind of an *analogical representation of fields:*

- It is based on a *grid (P,N)* where *V* is a set of selected points and N C *V* x *V* is a symmetric neighbourhood relation.
- It describes the spatial distribution of a parameter using a mapping / : *V* —> R of the points to the real numbers.
- It is specified extensionally (e.g. a matrix of floating point, numbers.)

Seismic simulators normally use regular grids obtained by rows and columns. They are characterized by a starting point s := (s_1, s_2)-, a unit distance A, the number n of columns and the number *m* of rows. The set of points is then given by

$$\mathcal{P} := \{(s_1 + i * \Delta, s_2 + j * \Delta) \mid i = 0, \ldots, n-1,\ j = 0, \ldots, m-1\} \quad (1)$$

Two points are neighbours if they have successive positions in the same row or column.

$$\mathcal{N} := \{(p, q) \in \mathcal{P} \times \mathcal{P} \mid |p - q| = \Delta\} \quad (2)$$

2.2 Histories of dynamic objects

Fields don't represent objects explicitly. They just show certain patterns of activity that are reproduced in the next instants. For example, figure 1 shows wave fronts that are propagating, hitting interfaces, and generating new waves. In order to describe these phenomena, we need an ontology for dynamic objects in fields.

Our discussion is based on a given (continuous) space S_1 for example the two-dimensional space defined by R^2, and a linear (continuous) time defined by T := R. Dynamic objects such as waves evolve in time and occupy a region at each time *t.* This region is a subset of *S* x *{t}.* If we consider different time points the occupied region of an object can change. We require that these changes are local. If we put the regions of an object at different times together, we obtain a subset of *S* x 7". This subset must be a 'connected piece of space-time', i.e. a *history* as defined in [Hayes, 1985b].

The region occupied by an object can change in a continuous or discontinuous way. For example, the initial

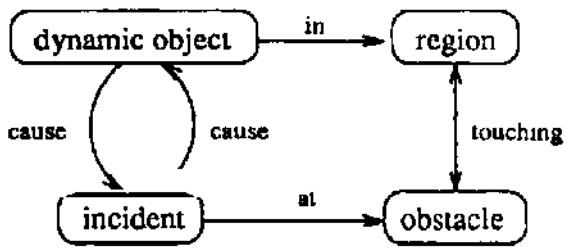

Figure 3: Ontological concepts for dynamic objects

wave front in figure 1 is split into two parts when hitting the interface. Changes are caused by the dynamic and the static field. In the case of seismic waves, discontinuities caused by the static field can be characterized precisely: If the velocities of a zone are changing continuously, a (convex) wave propagating through this zone will change continuously. Discontinuities in the velocity field however cause discontinuities in wave propagation.

In order to keep track of causes for discontinuous changes, we divide the static field into regions and obstacles. A *region* is a (maximal) coherent subset of S that does not contain discontinuities in the static field. The regions of the seismic velocity field are also called geological layers. An *obstacle* separates one, two, or several regions. It is a (maximal) coherent subset of S of discontinuity points in the static field. Its dimension is inferior to that of *S.* The geological model of figure 1 is composed of three 2D-regions of constant velocities, which are separated by three ID-obstacles called *interfaces.* The interfaces are linked by a corner which is a OD-obstacle. Regions, interfaces, and corners constitute a place vocabulary in the sense of [Hayes, 1985b; Forbus, 1994].

Thus, we divided the static field into regions where motion of dynamic objects is continuous and into obstacles which disturb motion in a discontinuous way. We now use this topological structure to divide the global histories into episodes of dynamic objects and incident events linking these episodes. We require that a dynamic object is contained into a single region. If it reaches an interface then the continuation of its history on the other side of the interface is considered to be a new object, namely the transmission of the incident object. A *dynamic object* is an episode of the global history that is contained in the static history of a certain region.

An *incident* is the event when a dynamic objects hits an obstacle. It is in fact the intersection of the history of the dynamic object with the history of the obstacle. The incident is caused by the incident object and causes itself new objects in the regions surrounding the obstacle. The global history is branching at the incidents as illustrated in figure 2. An incident is the start of the histories of the waves it causes and it links them with the history of the incident wave

Thus, we have structured histories in the dynamic fields into dynamic objects, incidents, and their causal relation. In fact, we have adapted the basic concepts of naive physics [Hayes, 1985b] to physical fields and now have a vocabulary for interpreting the simulated fields.

3 Interpreting snapshots

3.1 Detecting static histories

First we show bow to decompose the static velocity field into geological layers and interfaces. Thus, we obtain the regions where to look for waves and the obstacles where to look for incidents.

Let *{V,N)* be a grid and / : *V* — R be a field. We define regions as follows: let *C* C N be a symmetric criteria that specifies whether two neighbour points belong to the same region. We consider the reflexive transitive closure of *C* and denote it by *C.* *C** is the smallest superset of *C* that is reflexive and transitive. Since *C* is symmetric, *C* is an equivalence relation. The regions are obtained as the equivalence classes of C* The *C*-region of a point *p E V* is defined as the equivalence class containing ;>:

$$R_C(p) := \tilde{p}^{C^*} \tag{3}$$

To define regions in the velocity field *v* of seismic waves, we link two neighbour points if there is no discontinuity between them. Since grids have a fixed resolution, we use a threshold *i* to operationalize this criteria. The velocity difference of two points must be smaller than E*:*

$$V := \{(p,q) \in \mathcal{N} \mid |v(p) - v(q)| < \epsilon\} \tag{4}$$

The *geological layer* of point *p* is then the equivalence class *Fiv{p).*

Next we define interfaces separating two C-regions *R* and R_2 An interface is just a set of neighbourhood links *(p,q)* € N that do not satisfy the given criteria *C* and that connect a point in *R* with a point in *R2'.*

$$I_C(R_1, R_2) := ((R_1 \times R_2) \cap \mathcal{N}) - C \tag{5}$$

The set I(R_1,*R2)* is called C-interface between R_1 R_2 iff *1(R_1, R_2)* is not empty. The geological layers are separated by *V-interfaces.* For the sake of brevity, we neither discuss corners, nor the case that the interface between two regions is interrupted by a third region.

3.2 Detecting objects in a snapshot

In the next sections, we consider a sequence of snapshots $a_1, a_2, a_3, \ldots$ showing the amplitude field at increasing time points t_1, t_2, t_3 ■ ■ ■■ We proceed in three steps in order to detect histories of wave objects. First, we identify wave objects in a single snapshot. Then, we link the possible interpretations of succeeding snapshots. After that, we show how to detect histories of new objects caused by incidents at interfaces.

Wave fronts as shown in figure 1 consist of a small number of oscillations. In a snapshot, they appear as thin regions of negative or positive amplitudes, which can clearly be distinguished from the background having zero amplitude. To capture this phenomena formally, we divide the set *V* of points into three classes: *positive, negative,* and *zero* ones. Since there are small distortions in the simulated field, we use a $\delta > 0$ to define the zero class. Let a,- be the amplitude field of the *i-th* snapshot:

$$\begin{aligned} \mathcal{P}_i^+ &:= \{p \in \mathcal{P} \mid a_i(p) > \delta\} \\ \mathcal{P}_i^0 &:= \{p \in \mathcal{P} \mid -\delta \leq a_i(p) \leq \delta\} \\ \mathcal{P}_i^- &:= \{p \in \mathcal{P} \mid a_i(p) < -\delta\} \end{aligned} \tag{6}$$

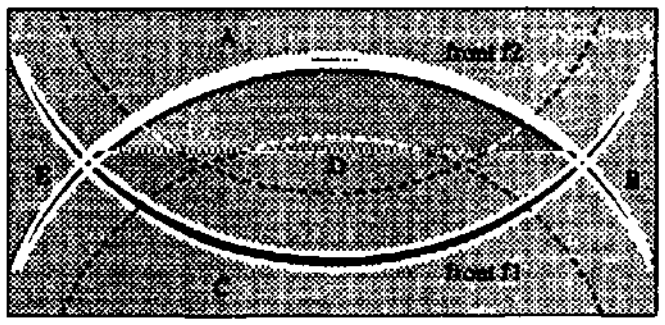

Figure 4: Two crossing fronts

Coherent regions of either positive, negative, or zero points are obtained by linking two neighbour points of the same class. Since we want to reconstruct wave fronts and each wave front is limited to a single geological layer we cut the regions in the amplitude field at the geological interfaces by using the criteria V.

$$A_i := V \cap \{(p,q) \in \mathcal{N} \mid \exists c \in \{-,+,0\} : p \in \mathcal{P}_i^c, q \in \mathcal{P}_i^c\} \quad (7)$$

This criteria A_i gives rise to A_i-regions and A_i-interfaces decomposing the geological layers at time t_i into positive, negative, and zero regions.

Characterizing wave fronts by their positive and negative regions is problematic because we can obtain intersections between several fronts (cf. figure 4). Due to this, the regions of several waves can merge. A more elegant and robust characterization is obtained by the zero regions that are enclosed by a wave. If a wave front f in the layer L is enclosing a zero region A then we obtain the front as the interface between the regions A and $L-A$. In case of interruptions, a front encloses several zero regions. Front f_1 in figure 4 encloses the zero regions A, D, whereas front f_2 encloses the regions D, C. f_1 also encloses the gap between the fronts A and D which is caused by f_2.

In order to close this gap, we will enlarge the zero regions of a layer L until the complete layer is covered. A single growing step adds the neighbouring layer points to a region $X \subseteq \mathcal{P}$:

$$grow(X) := X \cup \{p \in \mathcal{P} \mid \exists x \in X : (x,p) \in \mathcal{N} \cap V\} \quad (8)$$

We iterate this step until the layer L is completely covered. Let $\mathcal{Z}_i(L)$ be the set of the zero regions contained in the layer L at time t_i. The *i-th cover factor* of L is the smallest number k s.t.

$$L \subseteq \bigcup_{Z \in \mathcal{Z}_i(L)} grow^k(Z) \quad (9)$$

If Z is a zero region in layer L at time t_i and k is the cover factor of L at this time, then the *enlargement* of Z is defined as

$$\hat{Z} := grow^k(Z) \quad (10)$$

The enlargement enable us to define a wave front using the zero regions enclosed by it. Suppose that w is a wave in layer L and that the front of w at time t_i encloses[1] the zero regions $Z_1, \ldots, Z_m$ of L. Then

1. $\mathcal{Z}_i(w) := \{Z_1, \ldots, Z_m\}$ is called *i-the characterization of* w.
2. $from_i(w) := \hat{Z}_1 \cup \ldots \cup \hat{Z}_m$ is called the *i-th enclosed region of* w.
3. $to_i(w) := L - from_i(w)$ is called the *i-th propagation region of* w.

The interface between $from_i(w)$ and $to_i(w)$ represents the wave front. For example, the front f_1 is obtained as the interface between $\hat{A} \cup \hat{D}$ and $\hat{B} \cup \hat{C} \cup \hat{E}$, whereas f_2 is the interface between $\hat{C} \cup \hat{D}$ and $\hat{B} \cup \hat{A} \cup \hat{E}$.

If $from_i(w)$ is empty then the wave w has not yet appeared in snapshot i. If $to_i(w)$ is empty w has gone.

3.3 Tracking existing histories

Dynamic objects are steadily changing form and position. The time steps between two succeeding snapshots are usually too large to track these changes locally (cf. figure 1). In this section, we show how to track the history of an object even in presence of gaps.

For a given set $\mathcal{W}$ of waves and the set $\mathcal{Z}$ of zero regions of snapshot $i+1$, the task is to identify the $i+1$-th characterizations of the waves in $\mathcal{W}$ by using their i-th characterizations. We require that the new characterizations satisfy some additional criteria:

1. The new fronts should be in the propagation regions of the old fronts.
2. Each observed frontier between two zero regions should be explained by a wave.
3. The new fronts should be as close as possible to the old fronts.

The first constraint is based on the hypothesis that all points are propagating to the same side of the front. It implies that the enclosed region of a wave w is growing from one instant to the other, which is expressed by $from_i(w) \subseteq from_{i+1}(w)$. If a zero region $Z \in \mathcal{Z}$ of snapshot $i+1$ is overlapping with $from_i(w)$ it is also overlapping with $from_{i+1}(w)$ and therefore an element of the $i+1$-th characterization of w:

$$\text{if} \quad Z \cap from_i(w) \neq \emptyset \quad \text{then} \quad Z \in \mathcal{Z}_{i+1}(w) \quad (11)$$

The second constraint requires the detection of frontiers between two zero regions in a snapshot. In figure 4, D has a frontier with A and C, but not with B and E. If we let grow all regions then the borders of D will overlap with that of A, B, C, E. However, the overlap with B and E is also covered by the borders of A and C. This leads to the following definition: There is a *frontier* between two zero regions X and Y in $\mathcal{Z}$ iff

$$(grow(\hat{X}) \cap grow(\hat{Y})) - \bigcup_{Z \in \mathcal{Z} - \{X,Y\}} grow(\hat{Z}) \neq \emptyset \quad (12)$$

A frontier between X and Y is *explained* by a wave w iff w is enclosing exactly one of these zero regions, i.e. $|\{X,Y\} \cap \mathcal{Z}_{i+1}(w)| = 1$.

[1] Our characterization is based on the assumption that wave fronts always enclose a region. If a front ends inside a layer we can further divide the zero regions by lengthening this end.

These two constraints already reduce the number of possible interpretations. Consider figure 4 showing two waves w_1 and w_2 at two snapshots 1 and 2. Their wave fronts in snapshot 1 are indicated by dotted lines. The 1-st enclosed region of wave w_1 overlaps with the zero regions A and D, whereas the 1-st enclosed region of wave w_2 overlaps with C and D. Due to our first constraint, we get:

$$\{A, D\} \subseteq \mathcal{Z}_2(w_1) \qquad \{C, D\} \subseteq \mathcal{Z}_2(w_2) \tag{13}$$

In order to explain the frontier between C and D, the region C cannot be an element of $\mathcal{Z}_2(w_1)$. Similarly, A cannot be an element of $\mathcal{Z}_2(w_2)$. What about B and E? Their frontiers to the regions A and C are explained if they are not enclosed by wave w_1 and w_2. However, the frontiers of B are also explained if B is enclosed by w_1 and w_2. A similar argument holds for E. Thus, there are four characterizations explaining all frontiers:

$$\begin{array}{lll} 1. & \{A, D\} = \mathcal{Z}_2(w_1) & \{C, D\} = \mathcal{Z}_2(w_2) \\ 2. & \{A, D, E\} = \mathcal{Z}_2(w_1) & \{C, D, E\} = \mathcal{Z}_2(w_2) \\ 3. & \{A, D, B\} = \mathcal{Z}_2(w_1) & \{C, D, B\} = \mathcal{Z}_2(w_2) \\ 4. & \{A, D, B, E\} = \mathcal{Z}_2(w_1) & \{C, D, B, E\} = \mathcal{Z}_2(w_2) \end{array} \tag{14}$$

In order to reduce these ambiguities, we require that wave fronts are as close as possible to the old fronts. This can be achieved by minimizing the characterizations of waves. Let $\mathcal{Z}^1_{i+1} : \mathcal{W} \to 2^{\mathcal{Z}}$ and $\mathcal{Z}^2_{i+1} : \mathcal{W} \to 2^{\mathcal{Z}}$ be two characterizations. $\mathcal{Z}^1_{i+1}$ is *preferred* to $\mathcal{Z}^2_{i+1}$ iff

$$\mathcal{Z}^1_{i+1}(w) \subseteq \mathcal{Z}^2_{i+1}(w) \tag{15}$$

for each $w \in \mathcal{W}$. We don't accept a characterization $\mathcal{Z}'_{i+1}$ if there exists a characterization $\mathcal{Z}^*_{i+1}$ that is preferred and different to $\mathcal{Z}'_{i+1}$ and that satisfies the two constraints introduced above.

This eliminates the characterizations 2, 3, 4 of our example. Hence, the wave w_1 is characterized by $\{A, D\}$ and the wave w_2 is characterized by $\{C, D\}$. Our three principles are sufficient to track histories if the gaps between two succeeding fronts of a wave are not too large.

3.4 Detecting new histories

Intersections between different histories can be the start of new histories. In the case of seismic waves, the intersection of two wave histories is without interaction, whereas the intersection between a wave history and the static history of an obstacle bears new wave histories in the regions surrounding the obstacle. In this section, we show how to detect incidents and their resulting waves. For the sake of shortness, we consider only incidents at interfaces causing reflections and transmissions.

First, we discuss how to detect and characterize incidents to interfaces. Let w be a wave in layer L_1 and I be the (coherent) interface $I_V(L_1, L_2)$ between L_1 and a neighbouring layer L_2. The event of an incident of w to I is denoted by $e(w, I)$.

To detect an incident $e(w, I)$ in snapshot i, we are checking whether w hits I in this snapshot. A wave hits an interface iff the region behind it, as well as the region in front of it are touching this interface. A region $X \subseteq \mathcal{P}$ touches an interface $I \subseteq \mathcal{N}$ if some points of X are linked to other points by I. In this case, the following set of edges is non-empty:

$$touch(X, I) := \{(p, q) \in I \mid p \in X \text{ or } q \in X\} \tag{16}$$

We can now characterize incidents by the points in $to_i(w)$ and $from_i(w)$ that are touching I:

$$\begin{array}{rcl} from_i(e(w, I)) & := & touch(from_i(w), I) \\ to_i(e(w, I)) & := & touch(to_i(w), I) \end{array} \tag{17}$$

The set $from_i(e(w, I))$ is called the i-th *enclosed interface* of the incident $e(w, I)$, whereas $to_i(e(w, I))$ is called the i-th *propagation interface* of the incident $e(w, I)$.

If the i-th enclosed interface is empty then the incident $e(w, I)$ has not yet occurred in snapshot i. If the i-th propagation interface is empty then the incident is completed in snapshot i. If neither the i-th propagation interface, nor the i-th enclosed interface are empty then the incident *occurs* in snapshot i.

If an incident $e := e(w, I)$ occurs in a snapshot i then it causes a reflected wave $r(e)$ in the layer L_1 of the incident wave and a transmitted wave $t(e)$ in the layer L_2 on the other side of the interface. These waves exist if and only if the incident occurs:

$$\begin{array}{l} from_i(e(w, I)) \neq \emptyset \quad \text{iff} \quad from_i(r(e(w, I))) \neq \emptyset \\ from_i(e(w, I)) \neq \emptyset \quad \text{iff} \quad from_i(t(e(w, I))) \neq \emptyset \end{array} \tag{18}$$

The enclosed region of the reflected wave is touching the interface I exactly at the enclosed interface of the incident. Furthermore, the enclosed region of the reflected wave is included in the enclosed region of the incident wave:

$$\begin{array}{rcl} touch(from_i(r(e(w, I))), I) & = & from_i(e(w, I)) \\ from_i(r(e(w, I))) & \subseteq & from_i(w) \end{array} \tag{19}$$

The transmitted wave is touching the interface I at least at the enclosed interface of the incident:

$$touch(from_i(t(e(w, I))), I) \supseteq from_i(e(w, I)) \tag{20}$$

We don't get the inverse inclusion because the transmitted wave can be faster than the incident wave.

We are thus able to detect reflections and transmissions of existing waves, but we have not yet discussed how to detect the initial waves. Initial waves are obtained around a given source point $s \in \mathcal{P}$. Let L be the layer containing s. The initial wave w_0 encloses a zero region containing this source point provided the region does not cover the complete layer L:

$$\text{if} \quad Z \in \mathcal{Z}_i(L),\ s \in Z,\ Z \neq L \quad \text{then} \quad Z \in \mathcal{Z}_i(w_0) \tag{21}$$

As an example, we interpret the first and second snapshots of figure 1. Snapshot 1 decomposes layer L_1 into two zero regions A_{11}, A_{12} that are separated by a frontier. The region A_{11} contains the source point s. Hence, A_{11} is enclosed by the initial wave w_0. w_0 cannot enclose A_{12} because otherwise the frontier between A_{11} and A_{12} is not explained. Therefore, $\mathcal{Z}_1(w_0) = \{A_{11}\}$.

In the second snapshot, layer L_1 is divided into the zero regions $A_{21}, A_{22}, A_{23}, A_{24}$. The region A_{21} has frontiers with A_{22}, A_{23}, A_{24}. The old enclosed region of w_0 is overlapping with A_{21} and A_{22}. Hence:

$$\{A_{21}, A_{22}\} \subseteq \mathcal{Z}_2(w_0) \tag{22}$$

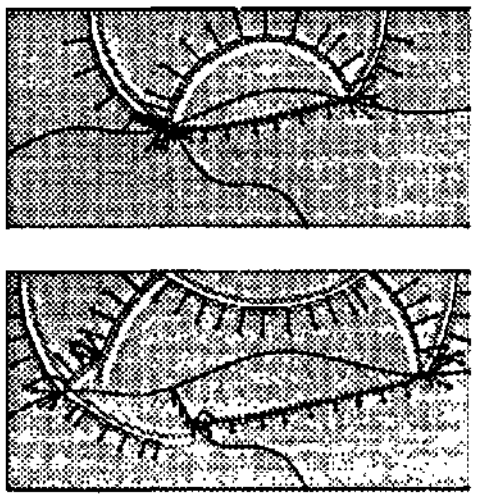

Figure 5: Wave fronts detected by the Sismonaute using rays

Region A_{22} is enclosed by w_0 and touching the interface I_1 between the layers L_1 and L_3. Therefore, the incident $e(w_0, I_1)$ occurs in snapshot 2 and the waves $r(e(w_0, I_1))$ and $t(e(w_0, I_1))$ exist in this snapshot. The reflected wave is in layer L_1 and its enclosed region is touching the interface I_1 at the enclosed interface of the incident. Therefore, the reflected wave contains the region A_{22}:

$$\{A_{22}\} \subseteq \mathcal{Z}_2(r(e(w_0, I_1))) \tag{23}$$

Layer L_3 is divided into the zero regions B_{21} and B_{22} which are separated by a frontier. B_{21} is touching the interface I_1 at the part that is touched by A_{22}. Since the transmitted wave is touching I_1 at the enclosed interface of the incident we get:

$$\{B_{21}\} \subseteq \mathcal{Z}_2(t(e(w_0, I_1))) \tag{24}$$

In order to explain all observed frontiers, the waves cannot enclose more regions as deduced above. Therefore, we get the following characterizations of waves:

$$\begin{array}{lcl} \mathcal{Z}_2(w_0) & = & \{A_{21}, A_{22}\} \\ \mathcal{Z}_2(r(e(w_0, I_1))) & = & \{A_{22}\} \\ \mathcal{Z}_2(t(e(w_0, I_1))) & = & \{B_{21}\} \end{array} \tag{25}$$

This example shows that it is possible to interpret snapshots by a qualitative analysis of zero regions and their neighbourhood relationships. This method can be extended to other kinds of waves such as diffracted waves. Problems are encountered if 1. fronts end in a region without enclosing it and 2. two fronts of a different origin are linked without showing an indication where this link can be found. In order to treat these problems, we need additional physical knowledge that cannot been extracted from the images. In [Junker, 1994], a wave front has been characterized by a sequence of rays called *polyray* (cf. figure 5). Polyrays provide the additional knowledge, but are difficult to manage when traversing curved interfaces. A compromise could be the use of two auxiliary rays marking the left and right ends of wave fronts to meet the problems of the qualitative interpretation method.

4 Related work

Recent work demonstrates the power of augmenting numerical simulation with qualitative notions. [Forbus and Falkenhainer, 1990] define the notion of *self-explanatory simulations* where the simulator itself is able to explain its behavior:

> a self-explanatory simulation integrates qualitative and numerical models to produce accurate predictions and causal explanations of the behavior of continuous physical systems.

They illustrate this definition with the SIMGEN program on physical systems simulated by ordinary differential equations.

Other examples of programs mixing quantitative simulation with qualitative notions can be found in the AI literature : the most famous being Q3 [Kuipers and Berleant, 1988], POINCARE [Sacks, 1991], the Kineticist's Workbench [Eisenberg, 1991], and others [Yip, 1987], [Zhao, 1991]. [Forbus, 1991] addressed an extension of qualitative reasoning to spatial information. In this work, Forbus advocates that, in order to be able to reason about, spatially distributed system, one needs to mix two representations which he calls a *metric diagram* (the quantitative part), and a *place vocabulary* (the symbolic part). The metric diagram is used for calculation whereas the place vocabulary is used for describing the system's behavior at a more abstract level, and for guiding the numeric computations which take place on the metric diagram. Moreover, these two representations are intertwined so that there is a correspondence between the places identified by the place vocabulary, and the quantities manipulated in the analog representation. In a more recent paper [Forbus, 1994], he proposes six challenge problems for spatial reasoning, the fourth one being :

> develop a system which can, given a sequence of weather maps for a region, provide a consistent qualitative explanation of the atmospheric behavior during that period ...

The problem we have addressed is very similar: Given a sequence of 2D snapshots of seismic amplitudes within the underground, our method provides a consistent qualitative explanation of the propagation of acoustic waves during that period. This has been achieved by effectively integrating several representations, namely a metric diagram (i.e. *fields)* used for simulation and a place vocabulary (i.e. *objects)* describing the geological structures. [junker, 1994] additionally experimented with a physical representation based on rays.

Research in qualitative and model-based reasoning has focused since its beginning on systems that could be simulated by ordinary differential equations (ODEs). Numerical simulators using differential equations can be divided into two classes: Those using scalar variables and those using field variables. Scalar variables describe different quantitative properties of a system and are not distributed over a space. Good examples of this class of systems are simple physical devices, chemical processes, chemical kinetics, global socio-economical models, or econometric models. In contrast to this, field

variables are distributed over a space, often related to the real world in one, two or three dimensions. Within this category, we can distinguish between fields of scalar variables and fields of vector variables. Different simulation techniques are used for approaching this kind of problems. Finite difference and finite elements are the conventional tools used by applied mathematicians for the simulation of field variables. Examples are fluid dynamics, geophysics or mechanics. Other approaches for field variables are naive physics and cellular automata, the basis for a number of ALife experiments such as Conway's game of life.

5 Conclusion

We developed a method for interpreting snapshot images produced by finite element, simulators for seismic wave propagation. As a result, the regions in the images are linked with Hayes-like histories of waves:

1. In order to detect wave fronts in a snapshot, we characterized them by the zero regions in the background they are enclosing. The first, snapshot contains a single front enclosing the zero region that contains the source point.
2. Symbolic constraints are posed on the zero regions to track a given wave from one snapshot to the other and to detect new waves. We obtain new waves when wave histories intersect with the static histories of obstacles.

A first prototype of a snapshot interpreter which is called SISMONAUTE [Junker, 1994] has been implemented using the ILOC tools LELISP, AIDA, and SMECI. This experience enabled us to find the crucial concepts for characterizing waves and for describing histories, as well as symbolic constraints, which enables the use of constraint programming tools to find globally consistent interpretations.

As a future perspective, the interpretation method could be adapted to other kinds of numerical simulations (e.g. that of flame fronts in simulations of combustions).

Acknowledgements

This work was initiated by Alain Bamberger (IFP) and significantly supported by Laurence Nicoletis, Laurent Anne, Jean Brae (IFP) and Michel Gondran (EDF). Furthermore, the authors would like to thank Claude Le Pape and the anonymous referees for their suggestions and comments.

References

[Anne and Brae, 1994] Laurent Anne and Jean Brac. 3D acoustic modelling software - B-version - Documentation and validation. Technical report, Institut Franc.ais du Petrole, Rueil-Malmaison, France, 1994,

[Eisenberg, 1991] M. Eisenberg. The kineticist's workbench : Combining symbolic and numerical methods in the simulation of chemical reaction mechanisms. Technical Report 1306, MIT Artificial Intelligence Laboratory, 1991.

[Forbus and Falkenhainer, 1990] K.D. Forbus and B. Falkenhainer. Self-explanatory simulations: An integration of qualitative and quantitative knowledge. In *Proceedings of the Eighth National Conference on Artificial Intelligence (AAAI-90),* pages 380-387. AAA! Press, 1990.

[Forbus, 1984] K. D. Forbus. Qualitative process theory. *Artificial Intelligence,* 24:85-168, 1984.

[Forbus, 1991] K.D. Forbus. Qualitative spatial reasoning. *Artificial Intelligence,* 51(3), 1991.

[Forbus, 1994] K. D. Forbus. Qualitative spatial reasoning: Framework and frontiers, report available by internet, Northwestern University, Evanston, IL, 1994.

[Fox, 1989] M. Fox. Knowledge-based simulation. In N. Nielsen L. Widman, K. Loparo, editor, *Artificial Intelligence, Simulation and Modeling.* Wiley Interscience, 1989.

[Hayes, 1985a] P.J. Hayes. Naive physics i: Ontology for liquids. In J, Hobbs and B. Moore, editors, *Formal Theories of the Commonscnse World,* pages 71-89. Ablex Publishing Corporation, 1985.

[Hayes, 1985b] P.J. Hayes. The second naive physics manifesto. In J. Hobbs and B. Moore, editors, *Formal Theories of the Commonscnse World,* pages 1-36. Ablex Publishing Corporation, 1985.

[Junker, 1994] U. Junker. Model-based reasoning meets 2I)-simulalions: Detecting physical wave phenomena in a series of snapshots. In *IA 94,* Paris, 1994. EC2.

[Kuipers and Berleant, 1988] B.J. Kuipers and D. Berleant Using incomplete quantitative knowledge in qualitative reasoning. In *Proceedings of the Seventh National Conference on Artificial Intelligence (AAAI 88),* pages 324-329. Morgan Kaufmann, San Mateo, CA, 1988.

[Lavergue, 1986] M. Lavergne. *Seismic methods.* Editions Technip et Institut Francais du Petrole, Paris, 198G.

[Sacks, 1991] E.P. Sacks. Automatic analysis of one-parainteter planar ordinary differential equations by intelligent numerical simulation. *Artificial Intelligence,* 48(1), 1991.

[Weld and de Kleer, 1990] D. S. Weld and J. de Kleer, editors. *Readings in Qualitative Reasoning About Physical Systems.* Morgan Kaufmann Publishers, San Mateo, CA, 1990,

[Yip, 1987] K.M. Yip. Extracting qualitative dynamics from numerical experiments. In *Proceedings of the Sixth National Conference on Artificial Intelligence (AAAI-87),* pages 665-671. Morgan Kaufmann, Los Altos, CA,, 1987.

[Zhao, 1991] F. Zhao. Extracting and representing qualitative behaviors of complex systems in phase spaces. In *Proceedings of the 18th International Conference on Artificial Intelligence,* pages 1144-1149. Morgan Kaufmann, Los Altos, CA,, 1991.